Immune factor of bacterial origin protects ticks against host microbial commensals

Authors: Beth M. Hayes[1†], Atanas D. Radkov[1†], Fauna Yarza[1], Sebastian Flores[1], Jungyun Kim[1], Ziyi Zhao[1], Katrina W. Lexa[2], Liron Marnin[3], Jacob Biboy[4], Victoria Bowcut[1], Waldemar Vollmer[4], Joao H. F. Pedra[3], Seemay Chou[1,5*].

Affiliations:

[1]Department of Biochemistry and Biophysics, University of California, San Francisco, San Francisco, CA 94158, USA.

[2]Modeling and Informatics, Denali Therapeutics, South San Francisco, CA, 94080, USA.

[3]Department of Microbiology and Immunology, University of Maryland School of Medicine, Baltimore, MD, USA.

[4]Centre for Bacterial Cell Biology, Biosciences Institute, Newcastle University, Newcastle upon Tyne, UK.

[5]Chan Zuckerberg Biohub, San Francisco, CA 94158, USA.

[†]These authors contributed equally.

*Correspondence to: seemay.chou@ucsf.edu

Abstract:

Disease vectors like hard ticks encounter diverse microbes while feeding on vertebrate hosts. We previously discovered that ticks horizontally acquired an antimicrobial toxin gene from bacteria known as *domesticated amidase effector 2* (*dae2)*. Here we show that this effector from *Ixodes scapularis* (Dae2^{Is}) is delivered to the host bite site via saliva and its structural and biochemical divergence from bacterial homologs expands targeting range to include host skin microbes. Disruption of *dae2^{Is}* increases the burden of skin-associated staphylococci within ticks, adversely affecting their fitness. In contrast, Dae2^{Is} has no intrinsic lytic activity against *Borrelia burgdorferi,* the tick symbiont that causes Lyme disease when transmitted to humans. Our observations suggest that ticks have evolved to preferentially resist their opportunistic pathogens, such as host skin commensals, while tolerating their own symbionts. These results highlight a unique interkingdom interface between blood-feeding vectors, hosts, and their associated microbes where incompatible host-microbe interactions lead to disease.

Main text:

Blood-feeding (hematophagy) arose independently in at least six different arthropod lineages approximately 50-150 million years ago (MYA), coincident with the emergence of a wide array of key host-modulating genes that support this specialized lifestyle[1-3]. The blacklegged tick *Ixodes scapularis* requires an especially prolonged, continuous bloodmeal in order to transition between each of its three life stages[4]. Ticks must establish an intimate attachment into the dermis of a bloodmeal host during this period for up to a week in length. To maintain this perilous yet essential interaction, ticks encode a cocktail of salivary molecules deployed at the bite site to block host immune and sensory responses while promoting blood flow[5-7]. Adapting to bloodmeal hosts also necessitates contending with host-associated microbes that can infect the tick or the tick bite site. Thus, the nature and selectivity of tick salivary activities provide a unique window into the evolutionary history of complex multi-kingdom interactions between ticks, their hosts, and microbes[6,8].

I. scapularis ticks employ a diverse repertoire of immune effectors, including antimicrobial peptides and lysozyme-like enzymes[9-11]. We previously found that *I. scapularis* and other ticks acquired a potent antibacterial enzyme approximately 40 MYA by domesticating an interbacterial competition toxin gene from bacteria[12]. The horizontally co-opted bacterial type VI secretion (T6S) amidase effector 2 (*tae2*) gene family encodes lytic cell wall-degrading enzymes delivered to rival Gram-negative bacteria by specialized bacterial T6SS machinery [13,14]. Tae2 toxins are hydrolases that break down the Gram-negative bacterial cell wall peptidoglycan (PG) of recipient microbes, resulting in osmotic stress and subsequent cell lysis. In contrast, the representative in ticks, domesticated amidase effector 2 (Dae2), does not have a specialized delivery system that allows it to cross the outer membrane of Gram-negative bacteria to access the PG and consequently is not intrinsically capable of gaining physical access to cell walls of Gram-negative bacteria due to their protective outer membrane[12]. Thus, it remains unknown whether Dae2 has been acquired by ticks to directly lyse bacteria. Nonetheless, given the rarity of interkingdom gene transfer and subsequent gene conservation[15], we hypothesize that Dae2 confers an adaptive fitness advantage to ticks. Therefore, we investigated the biological function of Dae2 and whether it affected microbes that ticks encounter during blood feeding

The microbiota of ticks are dominated by a few bacterial symbionts that are also transmissible human pathogens, including *Rickettsia spp.* and *Borrelia burgdorferi*, the causative agent of Lyme disease[16-21]. Our prior work revealed that *dae2*^{Is} modestly limits *B. burgdorferi* proliferation in *I. scapularis*[12]. Dae2^{Is} may prevent excessive *B. burgdorferi* proliferation that is detrimental to ticks. Alternatively, Dae2^{Is} could primarily target other bacteria in unknown ways, such as protecting against natural tick pathogens that have not been previously characterized. Here, we report that the structural and biochemical divergence of *I. scapularis*-encoded Dae2^{Is} from its ancestral bacterial counterparts broadens its antibacterial specificity, and extends its efficacy to Gram-positive bacteria, which lack an outer membrane and are enriched in the skin microbiota of mammals. Through its action in both the tick gut and saliva during feeding, Dae2^{Is} directly antagonizes bacterial commensals of bloodmeal host skin, which are detrimental to both the feeding success and viability of ticks.

Structural analysis of Tae2 and Dae2 enzymes

Evolutionary divergence of a gene following horizontal acquisition is driven by the biology of its recipient organism. A sequence-based comparison of the domesticated *dae2* genes from ticks and mites to ancestral bacterial *tae2* homologs showed several regions of variance between these groupings (Figure S1a-b). Although we were unable to definitively find evidence of positive or negative selection[12], these variances were unique to eukaryotic representatives and highly suggestive of functional differences, such as substrate specificity. To investigate this possibility, we determined the high-resolution structure of Tae2 from *Salmonella enterica* Typhi ($Tae2^{St}$) at a resolution of 2.05 Å by X-ray crystallography (Figure 1a, Table 1, PDB ID: 6WIN). $Tae2^{St}$ adopts a canonical papain-like amidase fold most similar to endolysin LysK from staphylococcal phage K (Figure S2)[22]. Structure-based alignment of threaded $Tae2^{St}$ and $Dae2^{Is}$ pointed to several key differences between eukaryotic and prokaryotic subgroups. Three major regions of sequence divergence mapped to the loops (L1-L3) that abut the catalytic channel (Figure 1b), This comparison also revealed substantial differences in the topology and electrostatic properties of a deep hydrophobic substrate-binding groove that extends from the active site (Figure 1c-d). The catalytic residues themselves are more accessible in $Dae2^{Is}$ than in $Tae2^{St}$, with a predicted pore behind the catalytic cysteine of $Dae2^{Is}$, which could provide substantial contact area for interactions with branched PG chains. Surface conservation profiles (Figure S3) further suggested that these divergent properties are conserved within Tae2 and Dae2 subgroups, respectively. Additionally, the catalytic channel for Dae2 is more open than that of Tae2. The differences in loop structures, the substrate-binding groove and the catalytic channel suggested that the substrate specificity of Dae2 could either be distinct or expanded from the bacterial enzymes.

Comparison of Tae2 and Dae2 cell wall specificities

The specificity of Dae2 for bacterial cell wall PG would dictate which microbes it can inhibit. We previously found that both Tae2 and Dae2 can hydrolyze Gram-negative cell walls[12]. Notably, PG chemical composition varies considerably between bacterial taxa, particularly at the third residue position within the peptide stem (Figure 2a)[23] For instance, Gram-negative bacteria incorporate *meso*-diaminopimelic acid (*m*DAP) at this variable third position, whereas bacteria from the class Bacillus have an amidated *m*DAP and other Gram-positive species have a lysine[23]. We hypothesized that this amino acid could influence Dae2 specificity, which we first investigated *in silico*. To compare substrate interaction surfaces, we computationally docked a fragment of crosslinked *m*DAP PG onto $Tae2^{St}$ and $Dae2^{Is}$ (Figure 2b-e). Docked PG adopted highly dissimilar poses between the two structures. We calculated an overall narrower cleft on $Tae2^{St}$ with 852.9 $Å^2$ active site surface area versus 1086.0 $Å^2$ for $Dae2^{Is}$, which also has an additional deep binding pocket. Upon binding, the cross-linked PG buried the binding surface significantly more in $Dae2^{Is}$ than $Tae2^{St}$, with a delta of 624.9 $Å^2$ compared to 450.2 $Å^2$. Our modeling and metadynamics simulations predicted a flipped PG orientation mediated through different residue interactions at the enzyme–substrate binding interface (Figure S3c-d) as well as tighter substrate binding.

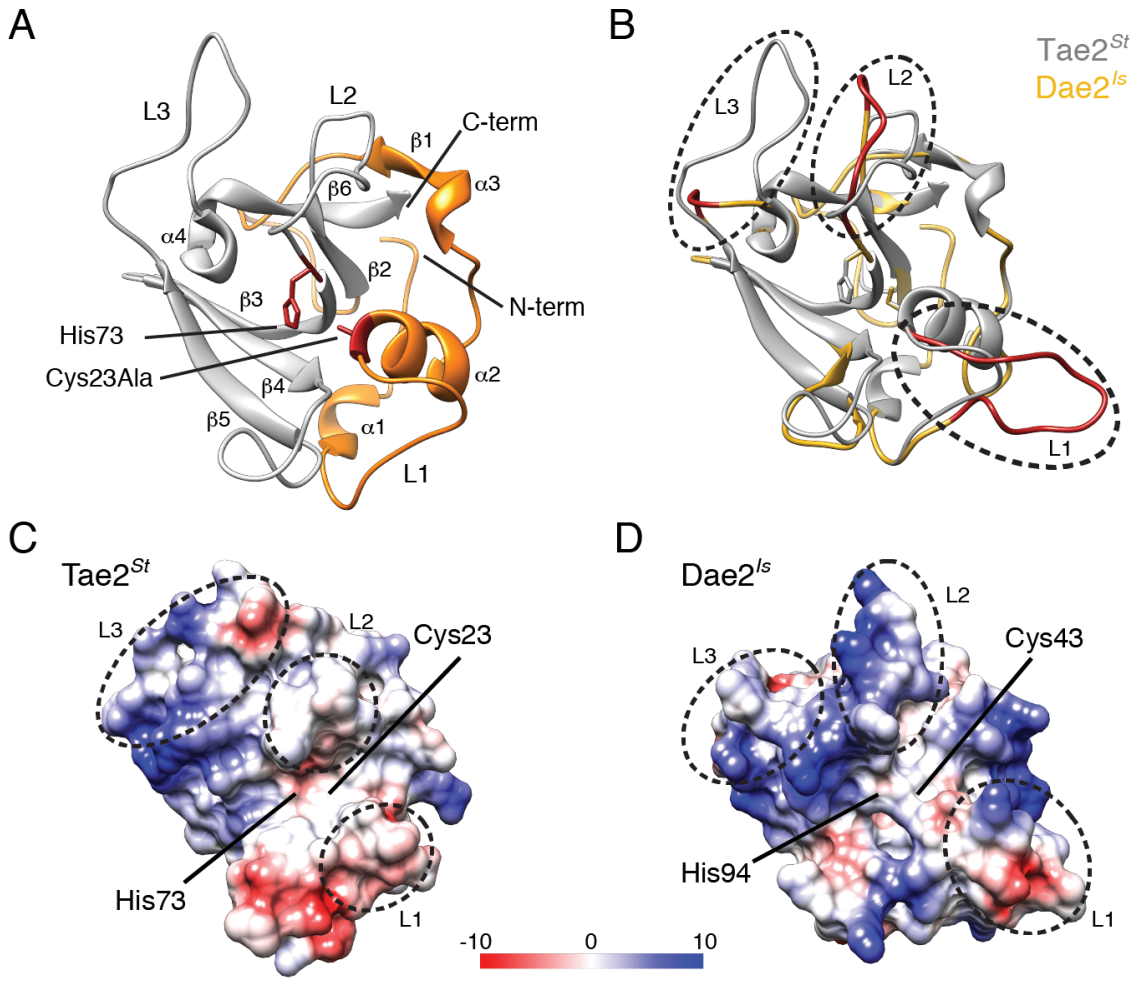

Figure 1: Comparison of Tae2 and Dae2 structures. (**A**) Ribbon diagram Tae2 from *Salmonella enterica* Typhi (Tae2St). Canonical papain-like secondary structures are labeled (α1-4, β1-6, Loop1-3 (L1-3)), and subdomains are colored (gray, orange). Catalytic residues are denoted (labeled His 73 and Cys23Ala, red). (**B**) Structural alignment of Tae2St (gray) and a Tae2-based model of Dae2^{ls} (golden). Loops 1, 2, and 3 are colored red in Dae2^{ls}. (**C, D**) Electrostatic charges in surfaces proximal to the catalytic residues for Tae2St (C) and Dae2^{ls} (D) (Scale is in kcal mol^{-1} e^{-1}). The loops are also boxed in the sequence alignment (Fig. S1).

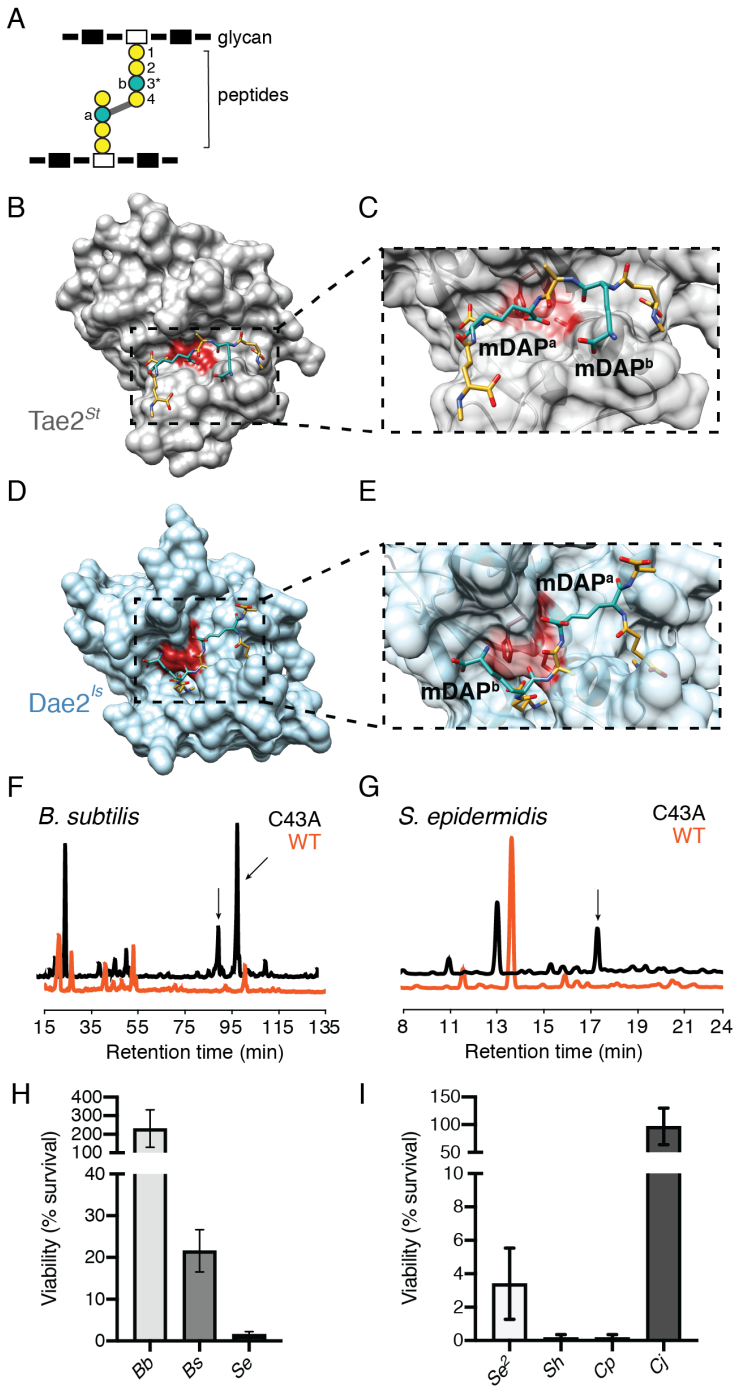

Figure 2: Enzymatic and antibacterial specificity of Tae2 and Dae2. (**A**) Cartoon schematic of bacterial peptidoglycan (PG) structure with glycans (rectangles), peptides (circles), and cross-link position (gray line) shown. Residue positions in PG peptide stem are labeled (1-4) with key variable third position (3*) colored in teal. (**B**) Surface representation of Tae2St ligand docking using a stem peptide substrate. Both *m*DAP residues in the stem peptide are colored in teal. (**C**) Close-up of the Tae2St active site and docked substrate. The scissile amide bond is between *m*DAP^{a} and the adjacent D-ala (position 4), proximal to the active site Cys23 residue. (**D**) Surface representation of Dae2^{Is} ligand docking, using the same substrate as for Tae2St in C. (**E**) Close-up of the Dae2^{Is} active site and docked substrate. The scissile bond is similarly situated between *m*DAP^{a} and the adjacent D-ala, proximal to the active site Cys43 residue. Notice the substrate directionality being *m*DAP^{b} – D-ala – *m*DAP^{a}, compared to the inverse for Tae2St, *m*DAP^{a} – D-ala – *m*DAP^{b}. HPLC chromatograms of PG from *B. subtilis* (**F**) and *S. epidermidis* (**G**) after enzymatic degradation with Dae2^{Is} wt (orange) and its catalytically inactive mutant (C43A, black). Arrows indicate the substrate peaks. Dae2^{Is} lysis assays of (**H**) Gram-negative *Borrelia burgdorferi* strain S9 (*Bb*), Gram-positive *Bacillus subtilis* 168 (*Bs*), and Gram-positive *Staphylococcus epidermidis* BCM060 (Se) and (**I**) Gram-positive skin associated bacteria *S. epidermidis* strain SK135 (*Se*^{2}), *S. hominis* strain SK119 (*Sh*), *Corynebacterium propinquum* DSM44285 (*Cp*) and *C. jeikeium* DSM7171 (*Cj*). Results are reported as percent survival with Dae2^{Is} wt normalized to its catalytic mutant C43A.

Altered binding and positioning of the PG substrate could affect activity against different cell wall types, which we hypothesized leads to a unique and potentially more promiscuous bacterial targeting range for Dae2 enzymes than their bacterial antecedents. In summary, our *in silico* modeling predicted that Dae2 enzymes can act on different PG structural groups than their bacterial Tae2 homologs, modifying or widening the range of bacteria they target.

To test this hypothesis, we comprehensively assessed the *in vitro* substrate specificity of Dae2^{Is} and Tae2St. We tested enzymes against a set of PG sacculi prepared from bacteria that we and others have found associated with field *I. scapularis* ticks: two environmental species (*Escherichia coli, Bacillus subtilis*) and a mammalian skin-associated bacterium (*Staphylococcus epidermidis*)[18,24]. Analysis of PG degradation by high performance liquid chromatography (HPLC) showed that the bacterial Tae2St-dependent hydrolysis was restricted to Gram-negative cell walls (Figure S4a-c), consistent with the restricted role Tae2 toxins play in contact-dependent T6S interbacterial competition specifically between Gram-negative bacteria. In contrast, Dae2^{Is} hydrolyzed all PG sacculi types tested (Figure 2f-g). Expansion of Dae2^{Is} activity to Gram-positive *S. epidermidis* PG was particularly remarkable, given how divergent its cell wall composition is from that of Gram-negative bacteria. These biochemical analyses raise the possibility that Dae2^{Is} has evolved to lyse a wider range of microbes.

Selectivity of Dae2^{Is} antimicrobial activity

To test whether the broadened specificity of Dae2^{Is} hydrolysis reflects broadened antibacterial activity, we assayed how Dae2^{Is} affects bacterial viability. We carried out bacterial killing assays at a physiologically relevant concentration of 2 μM Dae2^{Is}, a concentration chosen to be similar to that in dissected *I. scapularis* salivary glands (Figure S5). *E. coli* is intrinsically resistant to Dae2^{Is}, which is likely due to the inability of Dae2^{Is} to penetrate its outer membrane and access the PG[12]. Similarly, we found that Dae2^{Is} was not effective at killing the tick-borne spirochete *B. burgdorferi* (Figure 2h). *B. burgdorferi* also has an outer membrane, but it is highly distinct from that of *E. coli*[25,26]. Thus, any role of Dae2^{Is} against Gram-negative species is likely restricted to immunoregulatory processing of PG fragments or requires collaboration with another co-factor. In stark contrast, Dae2^{Is} is highly efficient at killing a strain of *S. epidermidis,* a human skin commensal, and moderately efficient at killing *B. subtilis,* a common environmental bacterium (Figure 2h), leading us to hypothesize that skin microbes, which are frequently encountered by feeding ticks, are targeted by Dae2^{Is}. We further tested Dae2^{Is} against three additional skin commensal species: another *S. epidermidis* strain, *S. hominis* and *Corynebacterium propiquum,* and observed immediate lysis of all (Figure 2i). Although related to *C. propiquum* and associated with human skin and mucus membranes, we did not observe killing of *C. jeikeium* by Dae2^{Is} (Fig. 2i), suggesting that Dae2^{Is} specificity is broad but not indiscriminate. It is possible that this more invasive strain of *Corynebacterium* has evolved mechanisms of resistance to cell wall targeting enzymes[27]. Together, our analyses led to two major conclusions. Together, our analyses revealed that expanded Dae2 specificity allows the eukaryotic enzymes to target a broader set of microbes than the prokaryotic Tae2 enzymes, and that Dae2 efficiently kills common skin commensals, which reside at the tick–host interface.

Localization of Dae2^{Is} during requisite bloodmeals

While feeding, ticks secrete a variety of salivary molecules to maintain bite site sterility and modulate host processes, such as immune and sensory responses (Figure 3a)[3,28]. We

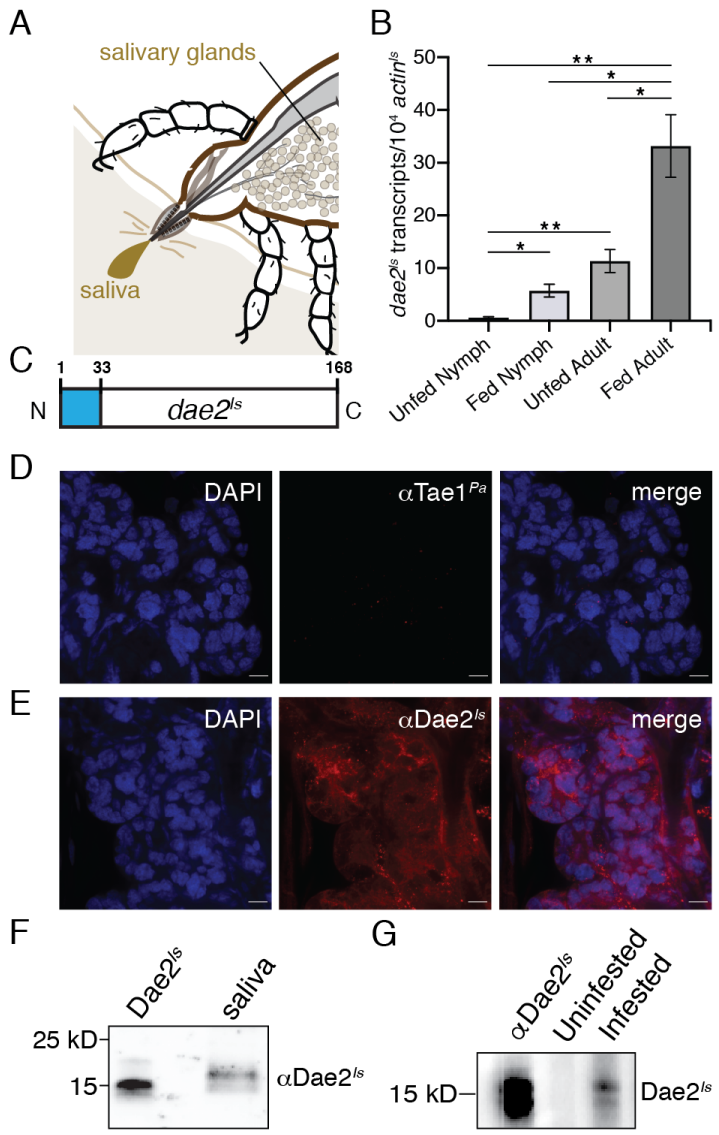

Figure 3: Regulation and localization of Dae2 in ticks during feeding. (**A**) Schematic of the tick at the bite-site interface showing the salivary glands. The salivary glands produce the saliva that is injected into the host. (**B**) *dae2*^{Is} expression (normalized against *actin*^{Is} transcripts) before (unfed) and after feeding (fed) on mice for nymph and adult ticks. * $p< 0.05$, ** $p<0.01$ (**C**) Diagram of the *dae2*^{Is} gene structure showing the predicted N-terminal signal sequence from nucleotide position 1-33 (blue) (**D-E**) Confocal images of *I. scapularis* salivary glands from adult females. Whole mounts were immunostained with DAPI (left panels, blue), control rabbit antibody against Tae1^{Pa} (D middle, red) or rabbit αDae2^{Is} (E middle, red). Scale bars= 15µm. More examples shown in Figure S6 (**F**) Western blot of collected saliva from partially fed *I. scapularis* adult females demonstrating presence of Dae2^{Is} in saliva. First lane has recombinant Dae2^{Is} as a positive control for rabbit αDae2^{Is} reactivity. (**G**) Western blot showing reactivity of mouse serum to Dae2^{Is}. Recombinant Dae2^{Is} protein was probed with mouse serum before (Uninfested) or after *I. scapularis* feeding (Infested). Rabbit αDae2^{Is} was used as positive control for reactivity (first lane).

hypothesized that ticks may have co-opted Dae2 to prevent bacterial contamination of host tissue and incoming bloodmeals. To begin to test this hypothesis, we examined Dae2^{Is} regulation and localization during feeding. We quantified *dae2*^{Is} transcripts in ticks before and after a bloodmeal and found dramatic upregulation of *dae2*^{Is} expression in both nymph and adult ticks following consumption of a bloodmeal (Figure 3b). It has also been shown previously that *dae2*^{Is} levels increase in response to *B. burgdorferi*-infected bloodmeals relative to uninfected bloodmeals[29]. Elevated levels of *dae2*^{Is} in feeding and infected ticks suggest an important functional role for Dae2^{Is} during this critical parasitic phase of the tick life cycle. The *dae2*^{Is} N-terminus is predicted to be a signal peptide (Figure 3c)[12], which suggests Dae2^{Is} could be secreted by tick salivary cells. Using immunofluorescence, we imaged Dae2^{Is} distribution in *I. scapularis* salivary glands by confocal microscopy and found that is localizes to vesicle-like puncta (Figure 3d-e, Figure S6). By immunoblot, we detected Dae2^{Is} in saliva harvested directly from partially-fed *I. scapularis* ticks (Figure 3f), suggesting Dae2^{Is} is secreted from vesicle-like structures into the saliva. The slight variation in protein size of Dae2 from ticks and the recombinant protein from *E. coli* might arise from posttranslational modification in the tick. Importantly, blood sera collected from mice that had been fed on by *I. scapularis* ticks (infested) showed immunoreactivity to Dae2^{Is}, and this was not the case for uninfested mice that had never been exposed to ticks (Figure 3g), indicating that the tick injects Dae2^{Is} into the bite site where it is recognized as an antigen for the murine immune system. From these results, we conclude that Dae2^{Is} is up-regulated during feeding and delivered to the bite site via saliva where it can physically access neighboring microbes, including bacteria that colonize host skin.

Importance of Dae2^{Is} for tick resistance to its own pathogens

Vertebrate host skin is colonized by microbial commensals that could infect the tick during feeding. Dae2^{Is} activity against skin bacteria suggested that Dae2 enzymes may help ticks resist these microbes. We therefore asked whether disruption of Dae2^{Is} in *I. scapularis* nymphs affects levels of skin-associated bacteria in ticks during feeding. We disrupted *dae2*^{Is} through microinjection-based RNA interference (RNAi) prior to feeding ticks on mice. In addition, we blocked pre-existing Dae2^{Is} protein stored in unfed tick salivary vesicles (Fig 3d-e and S6) using an antibody generated against recombinant Dae2^{Is} (αDae2^{Is}), which we found blocks lytic activity of the enzyme *in vitro* (Figure S7). 24 hours before tick feeding, we immunized host mice with αDae2^{Is}, which would inhibit Dae2^{Is} activity once delivered into the mice. Sterile saline was used as a control (Figure 4a). We retrieved ticks during the fast-feeding phase of their bloodmeals (day 3) and measured levels of skin-associated *Staphylococcus* present in ticks by qPCR. As a diversity of *Staphylococcus* commensal strains colonize mouse skin, we used genus-specific primers (Supplementary Table 2). Ticks from the experimental *dae2*^{Is} group supported higher levels of *Staphylococcus* bacteria than the control ticks (Figure 4b). We hypothesized that elevated levels of skin bacteria, such as *S. epidermidis*[20,31], might negatively impact tick health. Thus, we compared the feeding metrics of *dae2*^{Is} knockdown and control ticks feeding. We measured tick

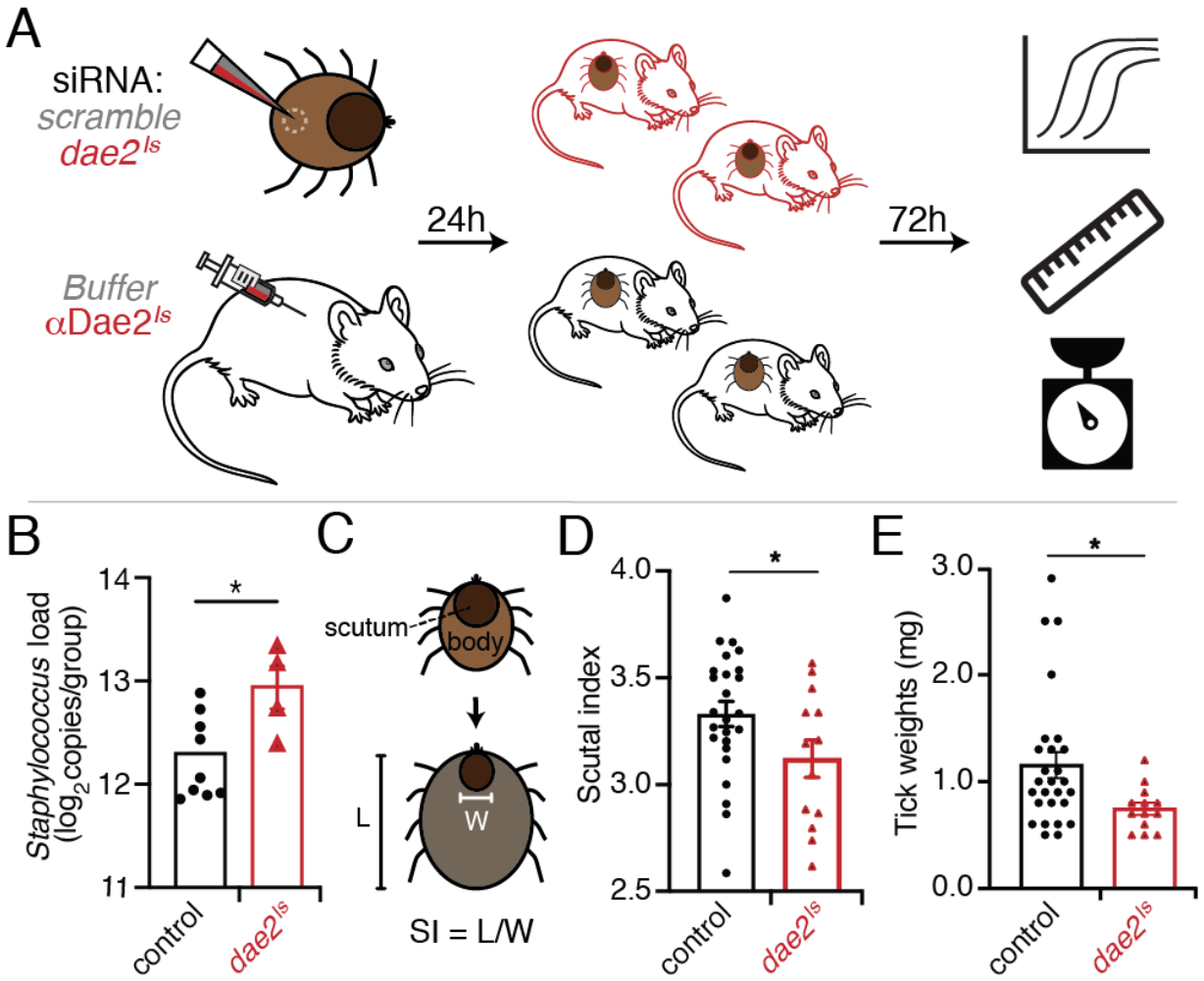

Figure 4: Dae2 activity affects tick fitness during feeding on mice. (A) Schematic of *in vivo* *dae2*^{Is} knockdown experiment. Mice were injected with sterile saline control (grey) or 2.5mg Rabbit αDae2^{Is} antibody and *I. scapularis* nymphs were microinjected with siRNAs targeting *dae2*^{Is} (red) or scrambled controls (grey). After 24 hour recovery, *dae2*^{Is} injected and scrambled injected ticks were placed on αDae2^{Is} antibody injected mice or control mice, respectively. Ticks were forcibly detached at 3 days and assessed by qPCR, scutal index, and weight. (**B**) *Staphylococcus* load was detected in DNA isolated from pooled *dae2*^{Is} knockdown (red) or control ticks (black) by qPCR with primers designed to target all species from the genus *Staphylococcus*. Results are presented as the average $\log_2$ *Staphylococcus* per tick. *$p<0.05$ with student's t-test. (**C**) Diagram of how scutal index (SI) changes during feeding. Scutal index is the ratio of the length of the entire tick body to the width of the scutum[30]. Scutal index (**D**) and tick weight (**E**) of individual ticks from experiment detailed in B. *$p<0.05$ based on student's t-test. Tick length and scutal width were measured from pictures with ImageJ. Weight was measured with an analytical balance with an error of +/- 0.1mg.

body expansion at day 3 by calculating scutal indices (SI), which reflect how long ticks have been feeding on a bloodmeal host (Figure 4c)[30]. Control ticks had significantly higher SI than *dae2*^{Is} knockdown ticks (Figure 4d). We also weighed individual ticks and found that *dae2*^{Is} ticks were lighter than controls (Figure 4e), suggesting increased host bacteria interfered with feeding. Impaired feeding may be due to slowed attachment, reduced blood intake, or some combination of these, ultimately resulting in decreased blood intake or more prolonged, hazardous interactions with a bloodmeal host.

Our previous experiment showed that reducing both secreted and endogenous Dae2^{Is} increased bacterial load, but did not directly address whether this enzyme directly kills *S. epidermidis* or other skin bacteria *in vivo*. In light of potent antibacterial activity we observe for Dae2^{Is} against skin microbes *in vitro*, we hypothesized that this enzyme directly kills *S. epidermidis* or other skin bacteria *in vivo*. Therefore, we assessed whether Dae2^{Is} can inhibit *S. epidermidis* inside of the tick by challenging ticks with *S. epidermidis*, coupled with biochemical inhibition of Dae2^{Is} activity. To inhibit this enzyme specifically within tick midguts, we took advantage of the inhibitory αDae2^{Is} antibody used in our *in vivo* knockdown experiments (Figure 4, Figure S7). We needle-challenged tick midguts with *S. epidermidis* with or without αDae2^{Is} and assessed whether depleting Dae2^{Is} activity specifically within the tick midgut affects *S. epidermidis* levels (Figure 5a). Co-injection of αDae2^{Is} with *S. epidermidis* led to higher levels of *S. epidermidis* in ticks than without the antibody at 4 hours post-injection, suggesting Dae2^{Is} has the capacity to directly antagonize *S. epidermidis in vivo* (Figure 5b) by killing or inhibiting the growth of cells. Interestingly, we also observed a concomitant increase in the death of the ticks themselves in the *Se*+αDae2^{Is} group (Figure 5c) compared to *Se* alone or the αDae2^{Is} control group. These effects demonstrate that there is a fitness cost to harboring high levels of *S. epidermidis*.

Based on these observations, we propose that bloodmeal host skin commensals are pathogenic to ticks and Dae2^{Is}-dependent inhibition of *S. epidermidis* promotes tick health. To our knowledge, our results identify the first known natural opportunistic pathogen of the tick disease vector *I. scapularis*. Future studies examining molecular and cellular changes at the host bite site will offer mechanistic insight into whether contamination of host tissues may also contribute to our observed phenotypes. Collectively, these data indicate that Dae2^{Is} confers the ability to resist diverse bacteria, including bloodmeal host skin commensals that are frequently and intimately encountered by ticks.

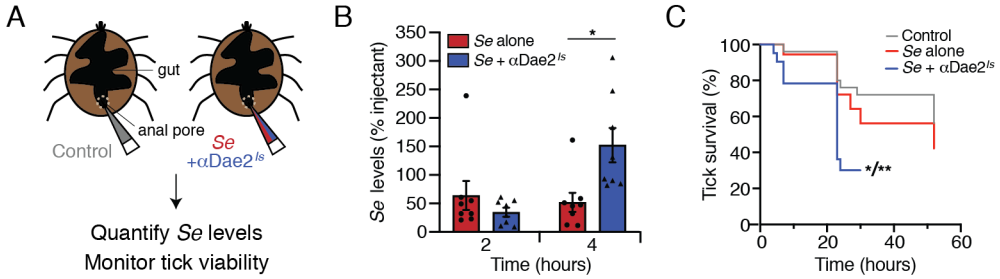

Figure 5: Dae2-dependent effects on *I. scapularis–S. epidermidis* interactions *in vivo*. (**A**) Schematic of experimental setup. *I. scapularis* nymphs were microinjected into the anal pore with a control antibody (grey, left), live *S. epidermidis* alone (red, right), or live *S. epidermidis* and $\alpha Dae2^{Is}$ together (blue, right). Ticks were then monitored for levels of *S. epidermidis* and tick survival. (**B**) CFU levels of *S. epidermidis* alone (red) or together with $\alpha Dae2^{Is}$ antibody to neutralize the lytic activity of $Dae2^{Is}$ (blue) at 2 and 4 hours post injection. Results are shown as percentage of CFU at time 0 (injectant). *$p<0.05$ based on paired t-test. (**C**) Tick survival after microinjection of $\alpha Dae2^{Is}$ control (grey), *S. epidermidis* alone (red), or *S. epidermidis* together with $\alpha Dae2^{Is}$ antibody to neutralize the lytic activity of $Dae2^{Is}$ (blue). *$p<0.05$ compared to *S. epidermidis* alone and **$p<0.01$ compared to antibody alone based on Log-rank (Mantel-Cox) test.

Discussion

Animals interact with diverse microbes, and whether a bacterium is beneficial or pathogenic is highly host-dependent [33]. Eukaryotes have evolved to respond appropriately; thus, the differential specificity of animal immune systems reflects how host–microbe interactions vary between organisms. Ticks harbor symbiotic microbes, such as *B. burgdorferi*, which are tolerated by their tick vector but are pathogenic to humans upon transmission[34]. In this study, we discovered that the opposite is also true: ticks are vulnerable to infection by bacterial commensals found on the skin of vertebrates they must feed on. Microbiota are important arms of animal physiology, and our observation that the domesticated tick immune factor Dae2 has evolved to target bacterial partners of vertebrate hosts highlights both the inseparability of these relationships and also the transmutable nature of microbial interactions across different biological contexts. Animals not only clash with each other but also with associated microbes, which are an integral part of an organismal "package." Particularly for blood-feeding parasites, such as ticks, successful navigation of these complex, interkingdom clashes is critical for survival.

This study revealed mechanisms by which the tick vector *I. scapularis* has evolved to mediate such a clash. The phylogenetic history of *dae2* as a horizontally transferred gene from bacteria granted us the unique opportunity to investigate how this immune effector has structurally, biochemically, and functionally diverged from its ancestral form to support the unique biology of ticks[12]. Invertebrates rely solely on innate immunity to distinguish between virulent and benign bacteria by employing pattern recognition receptors (PRRs) that recognize conserved microbe-associate molecular patterns (MAMPs), phagocytic cells, and a variety of humoral downstream effectors, including antimicrobial peptides (AMPs) and lytic enzymes[35-37]. These defense mechanisms can vary in their location, timing, and sensitivity to microbial signatures, contributing to the overall specificity of invertebrate–microbe interactions[38,39]. We discovered that Dae2^{Is} has evolved the capacity to selectively kill skin-associated bacteria of their bloodmeal hosts, and that these microbes pose a threat to tick health. The timing and location of Dae2^{Is} action in the saliva of ticks further contributes to its specific role in protecting against host microbes during feeding, suggesting this function is of biological importance to ticks.

Ticks have a very different relationship with its own symbiont *B. burgdorferi*, which stably colonizes the tick midgut and is maintained through a multi-host zoonotic lifecycle[4]. Although Dae2^{Is} does have the capacity to degrade purified *B. burgdorferi* PG, we did not detect direct killing of intact *B. burgdorferi.* We did, however, previously observe a modest but significant increase in *B. burgdorferi* levels in *dae2*^{Is} knockdown ticks[12]. The *I. scapularis* genome encodes functional homologs for several canonical innate immune signaling pathways [34,40], which can be activated through PG fragments. Thus, *dae2*-dependent inhibition of *B. burgdorferi* may have resulted from altered immune signaling in response to *B. burgdorferi* PG processing by Dae2^{Is}. Alternatively, Dae2^{Is} may act in synergy with an additional host factor, such as membrane-permeabilizing AMPs. Although limited, the ability of this effector to control a known symbiont may suggest that *I. scapularis* tolerance of *B. burgdorferi* is dependent on the ability of the tick to restrict *B. burgdorferi* proliferation to levels that are not detrimental to its own health.

More broadly, expansion of antimicrobial strategies was likely a key facilitator for the parasitic lifestyle of hematophagous arthropods. The rise of blood-feeding behavior over the

course of arthropod evolution was concomitant with the emergence of numerous antibacterial genes, such as *dae2*, that are expressed in saliva[41]. The intriguing timing of *dae2* acquisition by ticks and mites soon after the emergence of hematophagy within this arthropod clade[12] might indicate that Dae2 activity was an important enabler of blood-feeding. Hard ticks imbibe blood continuously from one host for several days at a time, leading to exceptionally intimate and sustained interactions with a wide range of vertebrates and associated microbes[42]. Our observations suggest that $dae2^{Is}$ ensures successful *I. scapularis* feeding by protecting ticks against infectious bacteria near host attachment sites. Antimicrobial activity in tick saliva could also provide a secondary benefit of blocking contamination of the bite site itself, preventing a cascade of antagonistic host responses. Hundreds of other tick salivary proteins await functional characterization[28,43,44] and will likely unveil novel aspects of relationships between hosts and this important class of disease vectors.

References

(1) Mans, B. J.; Neitz, A. W. H. *Insect Biochemistry and Molecular Biology* **2004**, *34* (1), 1–17.

(2) Mans, B. J. *JIN* **2011**, *3* (1), 41–51.

(3) Ribeiro, J. M.; Makoul, G. T.; Levine, J.; Robinson, D. R.; Spielman, A. *Journal of Experimental Medicine* **1985**, *161* (2), 332–344.

(4) Sonenshine, D. E. In *Tick-Borne Diseases of Humans*; American Society of Microbiology, 2005; pp 12–36.

(5) Ribeiro, J. M. C.; Francischetti, I. M. B. *Annu. Rev. Entomol.* **2003**, *48* (1), 73–88.

(6) Nuttall, P. A. *Wien. Klin. Wochenschr.* **2019**, *2528* (1), 1–12.

(7) Gillespie, R. D.; Mbow, M. L.; Titus, R. G. *Parasite Immunol.* **2000**, *22* (7), 319–331.

(8) Narasimhan, S.; Booth, C. J.; Deponte, K.; Wu, M.-J.; Liang, X.; Mohanty, S.; Kantor, F.; Fikrig, E. *Ticks Tick Borne Dis* **2019**, *10* (2), 386–397.

(9) Smith, A. A.; Pal, U. *Front Cell Infect Microbiol* **2014**, *4* (26), 116.

(10) Hajdušek, O.; Síma, R.; Ayllón, N.; Jalovecká, M.; Perner, J.; la Fuente, de, J.; Kopáček, P. *Front Cell Infect Microbiol* **2013**, *3*, 26.

(11) Kopáček, P. In *Encyclopedia of Parasitology*; Springer Berlin Heidelberg: Berlin, Heidelberg, 2015; pp 1–4.

(12) Chou, S.; Daugherty, M. D.; Peterson, S. B.; Biboy, J.; Yang, Y.; Jutras, B. L.; Fritz-Laylin, L. K.; Ferrin, M. A.; Harding, B. N.; Jacobs-Wagner, C.; Yang, X. F.; Vollmer, W.; Malik, H. S.; Mougous, J. D. *Nature* **2015**, *518* (7537), 98–101.

(13) Russell, A. B.; Hood, R. D.; Bui, N. K.; LeRoux, M.; Vollmer, W.; Mougous, J. D. *Nature* **2011**, *475* (7356), 343–347.

(14) Russell, A. B.; Singh, P.; Brittnacher, M.; Bui, N. K.; Hood, R. D.; Carl, M. A.; Agnello, D. M.; Schwarz, S.; Goodlett, D. R.; Vollmer, W.; Mougous, J. D. *Cell Host Microbe* **2012**, *11* (5), 538–549.

(15) Husnik, F.; McCutcheon, J. P. *Nature Reviews Microbiology* **2018**, *16* (2), 67–79.

(16) Tokarz, R.; Tagliafierro, T.; Sameroff, S.; Cucura, D. M.; Oleynik, A.; Che, X.; Jain, K.; Lipkin, W. I. *Ticks Tick Borne Dis* **2019**, *10* (4), 894–900.

(17) Díaz-Sánchez, S.; Hernández-Jarguín, A.; Torina, A.; de Mera, I. G. F.; Blanda, V.; Caracappa, S.; Gortazar, C.; la Fuente, de, J. *Ticks Tick Borne Dis* **2019**, *10* (2), 336–343.

(18) Ross, B. D.; Hayes, B.; Radey, M. C.; Lee, X.; Josek, T.; Bjork, J.; Neitzel, D.; Paskewitz, S.; Chou, S.; Mougous, J. D. *ISME J* **2018**, *12* (11), 2596–2607.

(19) Hernández-Jarguín, A.; Díaz-Sánchez, S.; Villar, M.; la Fuente, de, J. *Ticks Tick Borne Dis* **2018**, *9* (5), 1241–1251.

(20) Greay, T. L.; Gofton, A. W.; Paparini, A.; Ryan, U. M.; Oskam, C. L.; Irwin, P. J. *Parasit Vectors* **2018**, *11* (1), 12–14.

(21) Narasimhan, S.; Schuijt, T. J.; Abraham, N. M.; Rajeevan, N.; Coumou, J.; Graham, M.; Robson, A.; Wu, M.-J.; Daffre, S.; Hovius, J. W.; Fikrig, E. *Nat Commun* **2017**, *8* (1), 184–17.

(22) Sanz-Gaitero, M.; Keary, R.; Garcia-Doval, C.; Coffey, A.; van Raaij, M. J. *Virol. J.* **2014**, *11* (1), 133.

(23) Turner, R. D.; Vollmer, W.; Foster, S. J. *Molecular Microbiology* **2014**, *91* (5), 862–874.
(24) Narasimhan, S.; Fikrig, E. *Trends Parasitol.* **2015**, *31* (7), 315–323.
(25) Jutras, B. L.; Scott, M.; Parry, B.; Biboy, J.; Gray, J.; Vollmer, W.; Jacobs-Wagner, C. *Proc. Natl. Acad. Sci. U.S.A.* **2016**, *113* (33), 9162–9170.
(26) Jutras, B. L.; Lochhead, R. B.; Kloos, Z. A.; Biboy, J.; Strle, K.; Booth, C. J.; Govers, S. K.; Gray, J.; Schumann, P.; Vollmer, W.; Bockenstedt, L. K.; Steere, A. C.; Jacobs-Wagner, C. *Proc. Natl. Acad. Sci. U.S.A.* **2019**, *116* (27), 13498–13507.
(27) Bernard, K. *Journal of Clinical Microbiology* **2012**, *50* (10), 3152–3158.
(28) Kim, T. K.; Tirloni, L.; Pinto, A. F. M.; Moresco, J.; Yates, J. R.; da Silva Vaz, I.; Mulenga, A. *PLOS Negl Trop Dis* **2016**, *10* (1), e0004323.
(29) Smith, A. A.; Navasa, N.; Yang, X.; Wilder, C. N.; Buyuktanir, O.; Marques, A.; Anguita, J.; Pal, U. *Cell Host Microbe* **2016**, *20* (1), 91–98.
(30) Meiners, T.; Hammer, B.; Göbel, U. B.; Kahl, O. *Int. J. Med. Microbiol.* **2006**, *296 Suppl 40*, 103–107.
(31) Narasimhan, S.; Fikrig, E. *Trends Parasitol.* **2015**, *31* (7), 315–323.
(32) Dziarski, R.; Gupta, D. *Genome Biol.* **2006**, *7* (8), 232.
(33) Ehrlich, G. D.; Hiller, N. L.; Hu, F. Z. *Genome Biol.* **2008**, *9* (6), 225–227.
(34) Shaw, D. K.; Tate, A. T.; Schneider, D. S.; Levashina, E. A.; Kagan, J. C.; Pal, U.; Fikrig, E.; Pedra, J. H. F. *Trends Immunol.* **2018**, *39* (11), 862–873.
(35) Little, T. J.; Hultmark, D.; Read, A. F. *Nature Immunology* **2005**, *6* (7), 651–654.
(36) Schulenburg, H.; Boehnisch, C.; Michiels, N. K. *Mol. Immunol.* **2007**, *44* (13), 3338–3344.
(37) Humphreys, T.; Reinherz, E. L. *Immunology Today* **1994**, *15* (7), 316–320.
(38) Bosch, T. C. G.; Guillemin, K.; McFall-Ngai, M. *Bioessays* **2019**, *41* (10), e1800256.
(39) McFall-Ngai, M.; Hadfield, M. G.; Bosch, T. C. G.; Carey, H. V.; Domazet-Lošo, T.; Douglas, A. E.; Dubilier, N.; Eberl, G.; Fukami, T.; Gilbert, S. F.; Hentschel, U.; King, N.; Kjelleberg, S.; Knoll, A. H.; Kremer, N.; Mazmanian, S. K.; Metcalf, J. L.; Nealson, K.; Pierce, N. E.; Rawls, J. F.; Reid, A.; Ruby, E. G.; Rumpho, M.; Sanders, J. G.; Tautz, D.; Wernegreen, J. J. *Proc. Natl. Acad. Sci. U.S.A.* **2013**, *110* (9), 3229–3236.
(40) Gulia-Nuss, M.; Nuss, A. B.; Meyer, J. M.; Sonenshine, D. E.; Roe, R. M.; Waterhouse, R. M.; Sattelle, D. B.; la Fuente, de, J.; Ribeiro, J. M.; Megy, K.; Thimmapuram, J.; Miller, J. R.; Walenz, B. P.; Koren, S.; Hostetler, J. B.; Thiagarajan, M.; Joardar, V. S.; Hannick, L. I.; Bidwell, S.; Hammond, M. P.; Young, S.; Zeng, Q.; Abrudan, J. L.; Almeida, F. C.; Ayllón, N.; Bhide, K.; Bissinger, B. W.; Bonzon-Kulichenko, E.; Buckingham, S. D.; Caffrey, D. R.; Caimano, M. J.; Croset, V.; Driscoll, T.; Gilbert, D.; Gillespie, J. J.; Giraldo-Calderón, G. I.; Grabowski, J. M.; Jiang, D.; Khalil, S. M. S.; Kim, D.; Kocan, K. M.; Koči, J.; Kuhn, R. J.; Kurtti, T. J.; Lees, K.; Lang, E. G.; Kennedy, R. C.; Kwon, H.; Perera, R.; Qi, Y.; Radolf, J. D.; Sakamoto, J. M.; Sánchez-Gracia, A.; Severo, M. S.; Silverman, N.; Šimo, L.; Tojo, M.; Tornador, C.; Van Zee, J. P.; Vázquez, J.; Vieira, F. G.; Villar, M.; Wespiser, A. R.; Yang, Y.; Zhu, J.; Arensburger, P.; Pietrantonio, P. V.; Barker, S. C.; Shao, R.; Zdobnov, E. M.; Hauser, F.; Grimmelikhuijzen, C. J. P.; Park, Y.; Rozas, J.; Benton, R.; Pedra, J. H. F.; Nelson, D. R.; Unger, M. F.; Tubio, J. M. C.; Tu, Z.; Robertson, H. M.; Shumway, M.;

Sutton, G.; Wortman, J. R.; Lawson, D.; Wikel, S. K.; Nene, V. M.; Fraser, C. M.; Collins, F. H.; Birren, B.; Nelson, K. E.; Caler, E.; Hill, C. A. *Nat Commun* **2016**, *7*, 10507.

(41) disease, J. R. I. A. A.; 1995. *europepmc.org*.

(42) Sonenshine, D. E. *Biology of ticks. Vol. I*; 1991.

(43) Chmelař, J.; Kotál, J.; Karim, S.; Kopáček, P.; Francischetti, I. M. B.; Pedra, J. H. F.; Kotsyfakis, M. *Trends Parasitol.* **2016**, *32* (3), 242–254.

(44) Perner, J.; Kropáčková, S.; Kopáček, P.; Ribeiro, J. M. C. *PLOS Negl Trop Dis* **2018**, *12* (4), e0006410.

(45) Van Duyne, G. D.; Standaert, R. F.; Karplus, P. A.; Schreiber, S. L.; Clardy, J. *J. Mol. Biol.* **1993**, *229* (1), 105–124.

(46) MacDowell, A. A.; Celestre, R. S.; Howells, M.; McKinney, W.; Krupnick, J.; Cambie, D.; Domning, E. E.; Duarte, R. M.; Kelez, N.; Plate, D. W.; Cork, C. W.; Earnest, T. N.; Dickert, J.; Meigs, G.; Ralston, C.; Holton, J. M.; Alber, T.; Berger, J. M.; Agard, D. A.; Padmore, H. A. *J Synchrotron Radiat* **2004**, *11* (Pt 6), 447–455.

(47) Liebschner, D.; Afonine, P. V.; Baker, M. L.; Bunkoczi, G.; Chen, V. B.; Croll, T. I.; Hintze, B.; Hung, L. W.; Jain, S.; Mccoy, A. J.; Moriarty, N. W.; Oeffner, R. D.; Poon, B. K.; Prisant, M. G.; Read, R. J.; Richardson, J. S.; Richardson, D. C.; Sammito, M. D.; Sobolev, O. V.; Stockwell, D. H.; Terwilliger, T. C.; Urzhumtsev, A. G.; Videau, L. L.; Williams, C. J.; Adams, P. D. *Acta Crystallogr D Struct Biol* **2019**, *75* (10), 861–877.

(48) Emsley, P. **2017**.

(49) Holm, L.; Rosenström, P. *Nucleic Acids Res.* **2010**, *38* (Web Server issue), W545–W549.

(50) Pettersen, E. F.; Goddard, T. D.; Huang, C. C.; Couch, G. S.; Greenblatt, D. M.; Meng, E. C.; Ferrin, T. E. *J Comput Chem* **2004**, *25* (13), 1605–1612.

(51) Kelley, L. A.; Mezulis, S.; Yates, C. M.; Wass, M. N.; Sternberg, M. J. E. *Nat Protoc* **2015**, *10* (6), 845–858.

(52) Glauner, B. *Anal. Biochem.* **1988**, *172* (2), 451–464.

(53) Kolesnikova, T. D.; Semeshin, V. F.; Andreyeva, E. N.; Zykov, I. A.; Kokoza, E. B.; Kalashnikova, D. A.; Belyaeva, E. S.; Zhimulev, I. F. *Fly (Austin)* **2011**, *5* (3), 181–190.

(54) Rego, R. O. M.; Bestor, A.; Rosa, P. A. *J. Bacteriol.* **2011**, *193* (5), 1161–1171.

Acknowledgments: We are grateful to George Meigs and James Holton at the Advance Light Source (Lawrence Berkeley National Laboratory), the Stroud lab (UCSF) and Michael Thompson (Fraser lab, UCSF) for help with X-ray crystallography. We thank Carol Gross, Tiffany Scharschmidt and Joe Bondy-Denomy (all at UCSF) as well as Patricia Rosa (Rocky Mountain Laboratories, NIAID, NIH) for providing bacterial strains. We also appreciate Dyche Mullins and Samuel Lord (UCSF) for their assistance with microscopy. The Chou lab thanks Soraya Pedemonte and Ethel Enoex-Godonoo for lab and administrative help, respectively, without which the lab would not run as smoothly. We are also grateful to Harmit Malik (UCSF), Carol Gross (UCSF), Wallace Marshall (UCSF), Tiffany Scharschmidt (UCSF), Jeremy Reiter (UCSF), Thea Mauro (UCSF), and the entire Chou lab for helpful discussions and review of the manuscript.

Funding: This project was funded in part by NIH grants (R01AI132851 to SC, R01AI134696 to JP), Research Councils UK (EP/T002778/1) to WV, and UCSF Program for Breakthrough Biomedical Research, funded in part by the Sandler Foundation (to SC). Additional support for SC came from the Chan Zuckerberg Biohub the Johnson & Johnson WiSTEM2D Award. FY was supported by the National Science Foundation (1650113) and a grant to UCSF from the Howard Hughes Medical Institute through the James H. Gilliam Fellowships for Advanced Study program.

Author contributions: Conceptualization SC, BH, AR; Formal analysis KL; Funding acquisition SC, FY, JHFP, WV; Investigation BH, AR, FY, SF, JK, LM, JB, ZZ, VB; Methodology BH, AR, KL, WV, JHFP, SC; Project administration SC; Resources WV, KL, JHFP; Software KL; Supervision SC, WV, JHFP; Visualization SC, BH, AR, KL, ZZ; Writing (original draft) SC, BH, AR; Writing (review & editing) SC, BH, AR, JHFP, WV

Competing interests: Authors declare no competing interests.

Data and materials availability: Tae2St crystal structure data is available in the RCSB PDB database (PDB ID: 6WIN)